High-power tunable single-frequency 461 nm generation from an intracavity doubled Ti:sapphire laser with PPKTP

2016 Laser Phys. 26 025802

(http://iopscience.iop.org/1555-6611/26/2/025802)

IOP Publishing | Astro Ltd Laser Physics
Laser Phys. **26** (2016) 025802 (6pp) doi:10.1088/1054-660X/26/2/025802

High-power tunable single-frequency 461 nm generation from an intracavity doubled Ti:sapphire laser with PPKTP

Li Fengqin, Li Huijuan, Lu Huadong and Peng Kunchi

State Key Laboratory of Quantum Optics and Quantum Optics Devices, Collaborative Innovation Center of Extreme Optics, Institute of Opto-electronics, Shanxi University, Taiyuan 030006, People's Republic of China

E-mail: luhuadong@sxu.edu.cn

Received 1 September 2015, revised 8 November 2015
Accepted for publication 23 November 2015
Published 17 December 2015

Abstract

By optimising the resonator and choosing a periodically poled $KTiOPO_4$ (PPKTP) crystal as the doubler, a tunable single-frequency 461 nm laser with good performance is achieved. The output power at 460.86 nm and beam quality are of 1.05 W and better than 1.1, respectively. The measured linewidth is less than 590 kHz for 50 ms. By scanning the optical length of the resonator, the continuous frequency-tuning range of 15.756 GHz for the 460.86 nm laser is obtained.

Keywords: lasers, ring resonators, second harmonic generation, blue source

(Some figures may appear in colour only in the online journal)

1. Introduction

The research of optical atomic clocks based on the optical frequency standards of alkaline-earth atoms has become a new focus in recent years owing to their potential higher stability and accuracy [1]. Strontium atoms provide unique opportunities for research with narrow intercombination line transitions [2, 3]. The first stage of the laser cooling and trapping of strontium atoms based on the dipole transition from $^1S_0$ to $^1P_1$ state excited by the laser requires an available single-frequency blue laser at 460.86 nm with tunability [4]. The 460.86 nm laser with high power and good beam quality will be favourable for getting large atomic numbers, improving the capture rate, ensuring higher trapping and cooling efficiency and so on. Furthermore, the 461 nm laser mentioned here also facilitates other various experiments on ultracold neutral strontium atoms such as absorption imaging [5] and photo-associative spectroscopy (PAS) [6].

Presently the available lasers at 461 nm have been achieved by frequency-doubled laser diodes (LDs) [7–9]. With the development of the tapered amplifiers (TAs), the power of the LDs is drastically improved and the output power of the 461 nm lasers has also been improved up to 500 mW (Toptica Co, Ltd). Though the power of the 461 nm lasers can be increased with the assistance from the TAs, the output beam quality is poor and the intensity noise is relatively high, which limits their applications in atomic physics and so on. To compensate for the gap in the available commercial 461 nm lasers and to develop a blue laser source with a narrow linewidth, in 2005 Saenz realised a single-frequency 461 nm laser by an external-cavity frequency-doubled Ti:sapphire laser, where potassium niobate ($KNbO_3$) crystal was used as the frequency-doubler and the output power was only 125 mW [10]. In these external frequency-doubling experiments, the external cavities had to be locked to the input laser frequencies to obtain stable single-frequency 461 nm lasers, which increased the complexity of the laser systems. Compared to the external frequency-doubling, intracavity second-harmonic generation (SHG) by inserting a nonlinear crystal into the single-frequency Ti:sapphire laser resonator is an attractive approach to realising the 461 nm output owing to its compact structure and easy realisation. We realised a single-frequency intracavity doubled Ti:sapphire laser with the output wavelength of 461 nm [11] by using the BIBO (bismuth triborate, BiB_3O_6) crystal as the frequency-doubler. However, the output power was only 280 mW and the inevitable walk-off effect because of the critical phase-matching

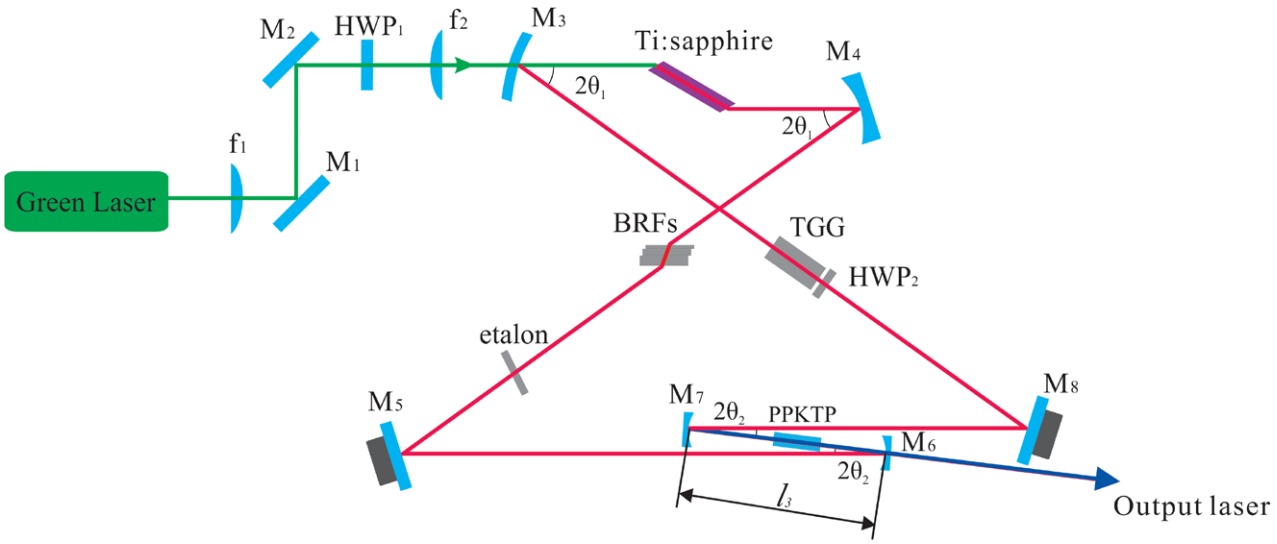

Figure 1. Experimental setup of the intracavity frequency doubled Ti:sapphire/PPKTP laser.

of the BIBO crystal decided that the output beam was elliptical, which limited its applications in lots of experiments. To improve the beam quality and get a high output power of over 1 W at 461 nm, in this paper we have chosen a PPKTP (periodically poled $KTiOPO_4$) crystal as the intracavity frequency-doubler, which has higher effective coefficient ($d_{\text{eff}} = 7.7 \times 10^{-12}$ m V^{-1}). By analysing the influence of the thermal-lens effect of the PPKTP due to the strong absorption of the generated 461 nm laser on the mode waist at the Ti:sapphire crystal, the curvatures of the resonator mirrors are optimised and a compact ring resonator with six mirrors is designed and built. When the length of the PPKTP is 18 mm and the central wavelength of the fundamental wave is finely tuned to be 921.72 nm, a 1.05 W single-frequency blue laser at 460.86 nm corresponding the absorption line of the strontium is generated with the pump power of 12 W and the greatly improved beam quality is measured to be $M^2 < 1.1$. The measured linewidth is less than 590 kHz for 50 ms. By means of the two piezo-electric transducers (PZTs) stuck on two plane mirrors, the continuously tuning range without mode-hopping for the fundamental and second-harmonic waves are 7.9 GHz and 15.8 GHz, respectively.

2. Experimental design and setup

The laser configuration and the experimental setup is illustrated in figure 1. A home-made all-solid-state single-frequency 532 nm laser (Yuguang Co, Ltd) with the highest output power of 12 W [12] is used as the pump source. The pump beam leaded by M_1 and M_2 is aligned and focused onto the Ti:sapphire crystal by a telescope coupling system which includes two lenses (f_1 and f_2) with focal lengths of 200 and 100 mm, respectively. A half wavelength plate (HWP_1) at 532 nm placed in front of the resonator can align the polarisation of the pump laser with respect to the optical axis of the Ti:sapphire crystal. The resonator with a ring configuration for the prevention of spatial hole burning is composed of six mirrors. To avoid introducing any additional divergence of

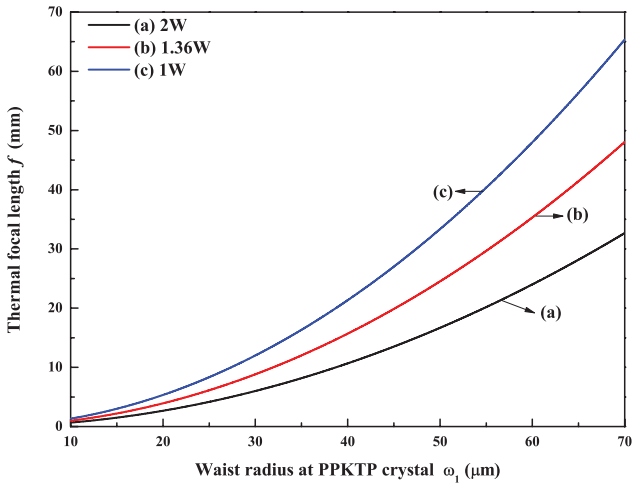

Figure 2. Thermal focal length of the PPKTP crystal versus the waist radius of fundamental-wave mode at the PPKTP crystal for different output powers. (a) $P = 2$ W, (b) $P = 1.36$ W, (c) $P = 1$ W.

the pump green laser, the input mirror M_3 is designed to be a meniscus concave mirror coated with high transmission films (HT) at 532 nm ($T > 95\%$) and high reflection (HR) films at 850 nm–950 nm ($R > 99.8\%$). M_4 is a plano-concave mirror coated with HR films at 850 nm–950 nm ($R > 99.8\%$). M_5 and M_8 are two plane mirrors coated with HR films at 850 nm–950 nm ($R > 99.8\%$). M_6 and M_7 are two plano-concave mirrors coated with HR films at 850 nm–950 nm ($R > 99.8\%$) and HT films at 461 nm ($T > 95\%$). The Brewster-angle (60.4°) cut Ti:sapphire crystal with a size of $\Phi 4$ mm $\times$ 20 mm is placed in the middle of M_3 and M_4. The absorption coefficient at 532 nm and figure of merit (FOM) are 1.0 cm^{-1} and 275, respectively. It is wrapped in indium foil and fixed in a water-cooled copper oven to efficiently remove the heat. A Faraday optical diode consisting of an 8 mm-long, 4 mm-diameter, terbium gallium garnet (TGG) rod positioned inside a stack of permanent Sm-Co ring magnets and a zeroth-order half wave-plate (HWP_2) coated with antireflection (AR) films at 600

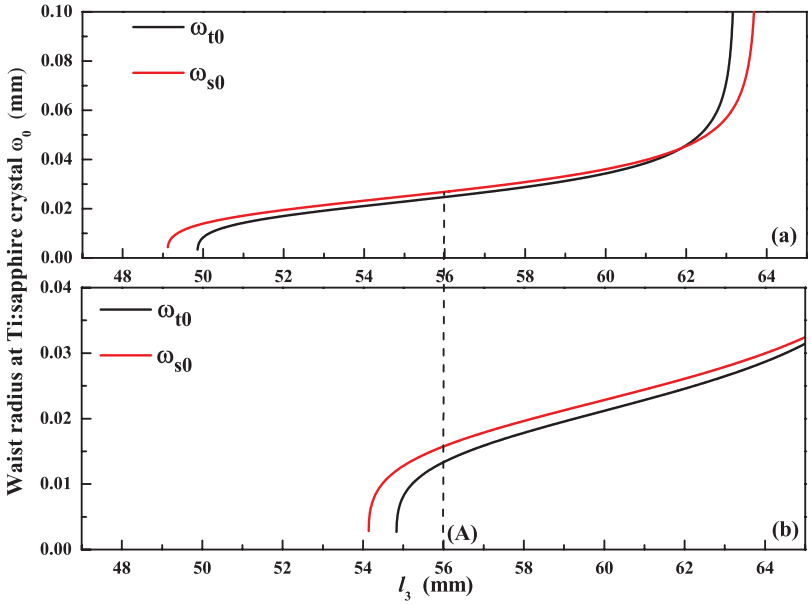

Figure 3. Radius of the waist at the Ti:sapphire crystal for M_6 and M_7 with the curvature radius of 50 mm. (a) Without the thermal-lens effect of the PPKTP, (b) with the thermal-lens effect of the PPKTP.

nm–1000 nm is inserted into the resonator to enforce unidirectional operation. A facet of the TGG crystal is 0.5°-wedged to effectively avoid the etalon effect. Three 1, 2 and 4 mm-thick BRFs are inserted into the cavity at a Brewster incident angle (57°) to coarsely tune the fundamental wavelength to be near 922 nm and meanwhile to narrow the bandwidth to be 4164 GHz. Finely frequency-tuning is realised by slightly rotating a 0.2 mm-thick uncoated etalon. The free spectral range (FSR) and finesse of the etalon are 517 GHz and 0.6, respectively. Moreover, the etalon can further effectively narrow the spectral bandwidth to be 244 GHz and maintain the reliable single-mode operation. To reduce the frequency drifting resulting from the surrounding temperature fluctuation, the etalon is precisely temperature controlled to be 25.00 °C. The continuously frequency tuning is realised by scanning the voltages of two PZTs (HPSt 500/10-5/7, Piezomechanik GmbH) stuck to both plane mirrors M_5 and M_8.

It is clear that the output power and the beam quality of the second-harmonic wave can be optimised by choosing a material that has a high effective nonlinear coefficient and is capable of noncritical phase matching (NCPM) to maximise the acceptance angle and minimise walk-off. Quasi-phase-matching (QPM) materials such as periodically poled $LiNbO_3$ (PPLN) and periodically poled $KTiOPO_4$ (PPKTP) [13, 14] can supply an attractive option for these applications. Compared to PPLN, an important advantage of PPKTP crystal is that KTP offers the possibility of quasi-phase-matching SHG at room temperature (although over 150 °C for PPLN) because the resistance to photo-refractive damage is greater than in $LiNbO_3$ [15]. However, the thermal-lens effect of the PPKTP crystal due to the absorption of the blue laser will badly influence the high efficiency and stable generation of the blue laser. So far, the research on the thermal-lens effect of the PPKTP crystal has been focused on the external cavity-enhanced SHG [7, 16, 17], where the thermal-lens effect of the PPKTP crystal cannot influence the oscillation of the fundamental-wave laser. To the best of our knowledge, there is no study on the thermal-lens effect of the PPKTP crystal in an intracavity-doubled Ti:sapphire laser, where the thermal-lens effect of the PPKTP crystal can not only influence the output power of the generated blue laser, but also directly influence the fundamental-wave oscillation. In our experiment, the adopted PPKTP crystal (Raicol Crystals Ltd) with a poling period of 5.55 μm is coated with AR films at 922 nm and 461 nm at both ends and positioned at the centre of M_6 and M_7. To implement the exact phase-matching of the PPKTP crystal, it is held inside a small brass oven which is mounted on a thermoelectric cooler (TEC) driven by a homemade high-precision temperature controller.

When the PPKTP crystal is adopted to act as the frequency-doubler for blue-UV laser, the thermal-lens effect caused by the strong absorption of blue-UV laser has to be taken into account. In order to achieve a stable blue laser at 461 nm with the high output power, we have to estimate the value of the thermal focal length, as shown in figure 2, according to the formula below [18],

$$f = \frac{\pi K_c \omega_T^2}{\eta P \frac{\mathrm{d}n}{\mathrm{d}t}} \frac{1}{1 - \exp(-\alpha l)}. \tag{1}$$

The parameters used to calculate the thermal focal length are thermal conductivity coefficient $K_c = 13$ $\mathrm{Wm^{-1}\ K^{-1}}$, thermo-optical coefficient $\mathrm{d}n/\mathrm{d}t = 1.6 \times 10^{-6}$ $\mathrm{K^{-1}}$, thermal conversion coefficient $\eta = 1$ and absorption coefficient $\alpha = 0.118\ \mathrm{cm^{-1}}$. Figure 2 shows that the thermal focal length increases not only with the increase in the waist radius at the PPKTP, but also with the decrease in the power of the blue laser. In order to alleviate the influence of the thermal-lens effect of the PPKTP crystal on the laser and to achieve the stable and high output power of the 461 nm laser, an effective method is to enlarge the waist radius of the fundamental-wave at the PPKTP.

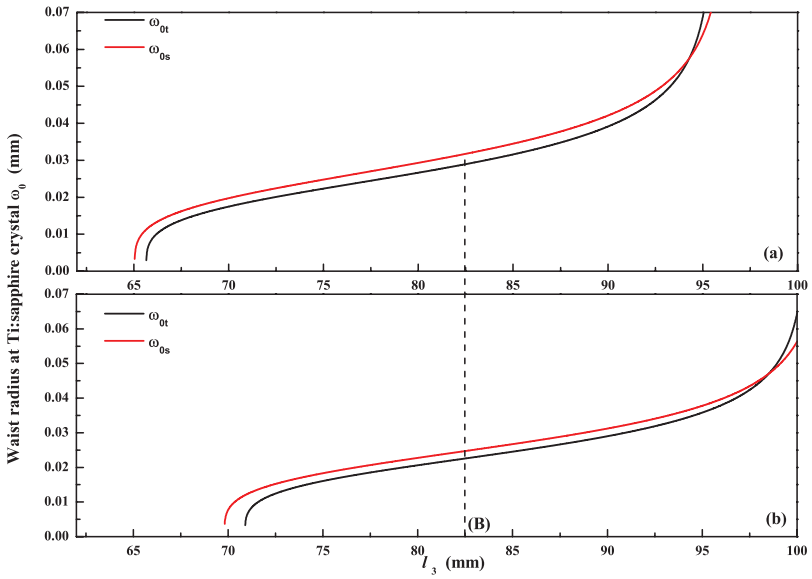

Figure 4. Radius of the waist at the Ti:sapphire crystal for M_6 and M_7 with the curvature radius of 75 mm. (a) Without the thermal-lens effect of the PPKTP, (b) with the thermal-lens effect of the PPKTP.

Further, we numerically calculate the waist of the Gaussian fundamental-wave at the Ti:sapphire crystal with and without the thermal-lens effect of the PPKTP for two different values of curvature radii of M_6 and M_7 by the ABCD matrix, which are shown in figures 3 and 4. The curvature radii of both M_3 and M_4 are fixed at 75 mm, and the length of the laser path outside M_6 and M_7 ($M_7 \rightarrow M_8 \rightarrow M_3 \rightarrow M_4 \rightarrow M_5 \rightarrow M_6$) is kept at 689 mm. The 17.5° incident angles of M_3 and M_4 can sufficiently compensate the astigmatism generated from the Brewster-cut Ti:sapphire crystal [19]. Figure 3 shows the functions of the waist radius at the Ti:sapphire crystal versus the length of the l_3 when the curvature radii of the M_6 and M_7 are 50 mm. Without considering the thermal-lens effect of the PPKTP crystal, the laser works at the centre of the stability range of the laser (Point (A) shown in figure 3(a)), where the length of l_3 equals 56 mm. Once the thermal-lens effect of the PPKTP crystal is taken into account, from figure 3 we can see that the thermal-lens effect of the PPKTP crystal can remove the laser to the edge of the stability range (Point (A) shown in figure 3(b)), and the optimal mode-matching between the pump and oscillating lasers will be broken, which can decrease the optical conversion efficiency and badly influence the intracavity power of the fundamental-wave laser. Finally, instability of the blue laser will occur. In order to obtain figure 3, the calculated waist radius at the PPKTP crystal and the thermal focal length of the PPKTP crystal are 32 μm and 10 mm, respectively (where the power of the blue laser is the experimental value of 1.36 W). However, when the curvature radii of the M_6 and M_7 are 75 mm, the corresponding calculated waist radius at the PPKTP crystal and the thermal focal length of the PPKTP crystal are enlarged to 47.5 μm and 22 mm, respectively. Without (Point (B) shown in figure 4(a)) and with (Point (B) shown in figure 4(b)) the thermal-lens effect of the PPKTP crystal, the laser can both work at the centre of the stability range, which is shown in figure 4. At that time, the mode-matching is still kept and we can obtain the stable blue output laser.

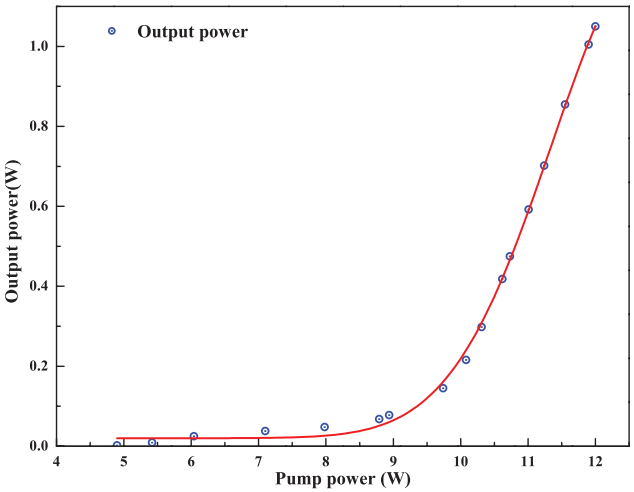

Figure 5. Output power of 461 nm laser versus the incident pump power.

3. Experimental results

By rotating the BRFs and changing the incident angle of the etalon, the central wavelength is tuned to be 921.72 nm, which corresponds to the SHG at 460.86 nm for strontium laser cooling and trapping. When the curvature radii of the M_6 and M_7 are 50 mm, the blue laser can flash before one and rapidly drop. However, when the M_6 and M_7 with the curvature radius of 75 mm is adopted, the stable 461 nm laser with 1.05 W is obtained. Figure 5 shows the output power curve with the pump power. It is clear that the threshold pump power is about 4 W and the maximal blue output power of 1.05 W with single-frequency operation is obtained at the incident pump power of 12 W. The maximal optical–optical conversion efficiency is 8.75% from 532 nm to 460.86 nm.

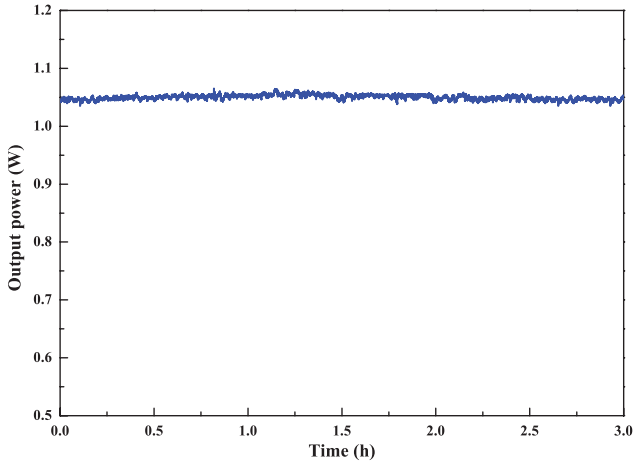

Figure 6. Long-term power stability of 461 nm laser for 3 h.

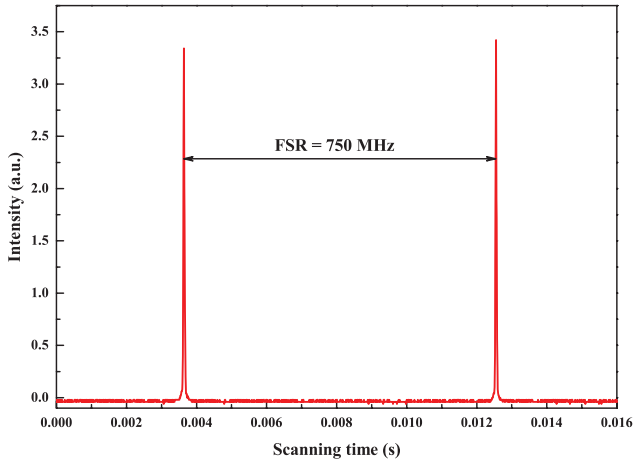

Figure 7. Longitudinal-mode structure of the laser by scanning the confocal F–P cavity.

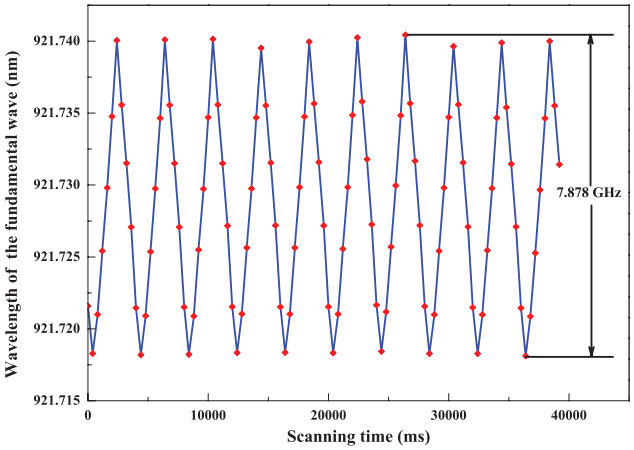

Figure 8. Automatic scanning frequency of the laser.

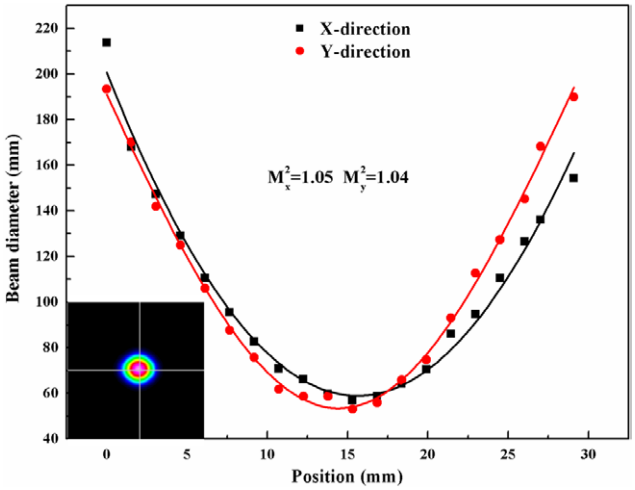

Figure 9. Measured M^2 values and the spatial beam profile for a 461 nm laser.

No obvious gain saturation phenomenon depicts that the thermal effect of PPKTP crystal induced by absorbing of blue laser has been effectively avoided by loose focus at the PPKTP crystal under the pump power of 12 W. At this moment, the optimum phase-matching temperature of PPKTP is scanned to be 32.50 °C, which is slightly higher than the theoretical calculated value 26.50 °C [20, 21]. The reason is the non-perfect alignment between the fundamental beam and crystal axis for our conscious misalignment with a small tilt angle at the incident plane of PPKTP to avoid the etalon effect resulting from the two plane surfaces. The long-term power stability at 460.86 nm recorded by a power meter is better than ±1.5% over three h, as shown in figure 6. At the same time, a small part of the fundamental output power is injected into a Fabry–Perot interferometer to monitor the property of single-mode operation of the laser system, as shown in figure 7, which shows that the laser can operate in the single-longitudinal mode. The main contribution is attributed to the SHG process, which introduces sufficient nonlinear loss for the nonlasing mode and naturally suppresses the multi-longitudinal mode oscillation, as mentioned in [22, 23]. On the basis of nonlinear loss theory for single-mode operation, a continuous tuning-range of 7.878 GHz nearly 921.72 nm without mode-hopping is further realised by scanning the cavity optical length via two PZTs stuck to M_5 and M_8 mirrors, as shown in figure 8. Correspondingly, the continuous tuning range of the second-harmonic wave at 460.86 nm is 15.756 GHz. The continuous frequency-tuning range is broad enough to satisfy the requirement of the experiments for probe narrow strontium atomic transitions. The beam quality of the blue laser, which is also one of the important parameters we are focused on, has been improved greatly to be a good Gaussian beam. This is measured by a M^2 meter (M2DU, DataRay Inc.) and the measured values of M_x^2 and M_y^2 are 1.05 and 1.04, respectively. The measured caustic curve and the corresponding spatial beam profile are shown in figure 9 and its inset, respectively. Finally, a small part of the laser is injected into an F–P interferometer with high accuracy to measure the linewidth of the obtained laser, and the measured value is less than 590 kHz for 50 ms.

4. Conclusions

In summary, we have realised a CW tunable single-frequency 461 nm laser with high output power and perfect beam quality by means of an intracavity-doubled Ti:sapphire laser with a

PPKTP crystal. We first analysed the influence of the thermal-lens effect of the PPKTP crystal on the waist radius of the laser at the Ti:sapphire crystal, and optimised the curvature radii of the cavity mirrors. Then an insensitive resonator to the thermal-lens effect of the PPKTP crystal was designed and constructed, and a single-frequency 461 nm laser with an output power of 1.05 W was obtained. The optical–optical conversion efficiency from the 532 nm laser to the 461 nm laser was 8.75%. The measured long-term power stability and beam quality were better than $\pm 1.5\%$ over 3 h and 1.1, respectively. The maximal continuous tuning range of 15.756 GHz at 460.86 nm without mode-hopping was obtained by scanning the voltage of two PZTs. For the first time we have realised this high-power, all-solid-state CW blue laser at 461 nm with good beam quality, and we believe that the obtained laser is a high potential light source for strontium laser trapping and cooling, especially for other various experiments on ultracold neutral strontium such as absorption imaging and PAS.

Acknowledgments

This research was supported in part by the National Natural Science Foundation of China (Grant No. 61405107, 11504220, 61227902, 61227015), Natural Science Foundation of Shanxi Province (Grant No. 2014021011-3).

References

[1] Hong T, Cramer C, Nagourney W and Fortson E N 2004 *Phys. Rev. Lett.* **94** 050801
[2] Tarrallo M G 2009 *PhD Thesis* Galileo Galilei School
[3] Santra R, Arimondo E, Ido T, Greene C H and Ye J 2005 *Phys. Rev. Lett.* **94** 173002
[4] Xu X, Loftus T H, Hall J L, Gallagher A and Ye J 2003 *J. Opt. Soc. Am.* B **20** 968–76
[5] Simien C E, Chen Y C, Gupta P, Laha S, Martinez Y N, Mickelson P G, Nagel S B and Killian T C 2004 *Phys. Rev. Lett.* **92** 143001
[6] Nagel S B, Mickelson P G, Saenz A D, Martinez Y N, Chen Y C, Killian T C, Pellegrini P and Cote R 2005 *Phys. Rev. Lett.* **94** 083004
[7] Le Targat R, Zondy J C J and Lemonde P 2005 *Opt. Commun.* **247** 471–81
[8] Woll D, Schumacher J, Robertson A, Tremont M A and Wallenstein R 2002 *Opt. Lett.* **27** 1055–7
[9] Schwedes C H, Peik E, Von Zanthier J, Nevsky A Y and Walther H 2003 *Appl. Phys.* B **76** 143–7
[10] Saenz A D 2005 *Master's Thesis* Rice University
[11] Li F Q, Shi Z, Li Y M and Peng K C 2011 *Chin. Phys. Lett.* **28** 124205
[12] Wang Y J, Zheng Y H, Shi Z and Peng K C 2012 *Laser Phys. Lett.* **9** 506–10
[13] Krzempek K, Sobon G, Sotor J, Dudzik G and Abramski K M 2014 *Laser Phys. Lett.* **11** 105103
[14] Chunchumishev D, Marchev G, Buchvarov I, Pasiskericius V, Laurell F and Petrov V 2013 *Laser Phys. Lett.* **10** 115404
[15] Pierrou M, Laurell F, Karlsson H, Kellner T, Czeranowsky C and Huber G 1999 *Opt. Lett.* **24** 205–7
[16] Liao Z M, Payne S A, Dawsonn J, Drobshoff A, Ebbers C and Pennington D 2004 *J. Opt. Soc. Am.* B **21** 2191–5
[17] Yang W H, Wang Y J, Zheng Y H and Lu H D 2015 *Opt. Express* **21** 19624–33
[18] Innocenzil M E, Yural H T, Fincherl C L and Fields R A 1990 *Appl. Phys. Lett.* **56** 1831–3
[19] Sun Y, Lu H D and Su J 2008 *Acta Sin. Quantum Opt.* **14** 344–7
[20] Fradkin K, Arie A, Skliar A and Rosenman G 1999 *Appl. Phys. Lett.* **74** 914–6
[21] Emanueli S and Arie A 2003 *Appl. Opt.* **42** 6661–5
[22] Lu H D, Su J, Zheng Y H and Peng K C 2014 *Opt. Lett.* **39** 1117–20
[23] Lu H D, Sun X J, Wang M H, Su J and Peng K C 2014 *Opt. Express* **22** 24551–8